Ritari, Antti; Huotari, Janne; Tammi, Kari

Marine vessel powertrain design optimization: Multiperiod modeling considering retrofits and alternative fuels

Published in:
Proceedings of the Institution of Mechanical Engineers Part M: Journal of Engineering for the Maritime Environment

DOI:
10.1177/14750902221145747

Published: 01/08/2023

Document Version
Publisher's PDF, also known as Version of record

Please cite the original version:
Ritari, A., Huotari, J., & Tammi, K. (2023). Marine vessel powertrain design optimization: Multiperiod modeling considering retrofits and alternative fuels. *Proceedings of the Institution of Mechanical Engineers Part M: Journal of Engineering for the Maritime Environment*, *237*(3), 597-614. https://doi.org/10.1177/14750902221145747

Marine vessel powertrain design optimization: Multiperiod modeling considering retrofits and alternative fuels

Antti Ritari[1], Janne Huotari[1] and Kari Tammi[1]

Abstract

Over the coming decades, maritime transportation will transition from fossil hydrocarbon fuels to hydrogen, ammonia, and synthetic hydrocarbon fuels produced using renewable electricity as the primary energy source. In this context, a shipowner needs to identify a cost-efficient plan for the adoption of alternative fuels and onboard energy conversion system retrofits. This paper presents a multiperiod decision model for the selection of energy system components under increasingly stringent CO_2 emissions regulations and cost forecasts over a multidecade planning horizon. The model considers the choice of newbuild architecture, timing of retrofits, component sizes, and allocation of fuels to converters with the objective of minimizing total cost of ownership (TCO). The decision problem is formulated as a discrete time multiperiod mixed-integer linear program. The application of the model is numerically illustrated for a Baltic Sea roll-on/roll-off ferry. The main findings are: (i) modifying the energy system with retrofits obtains 41% lower TCO compared to fuel switching alone; (ii) batteries contribute to 23% lower TCO; (iii) optimal component installation period can be shorter than their maximum lifetime; (iv) running an engine with hydrogen is favoured over fuel cells and (v) shaft electric machine is the key design choice enabling energy system flexibility.

Keywords

lifecycle evaluation, emission abatement, energy efficiency, ship design, design optimization, integer programming, energy storage, synthetic fuels, hydrogen

Introduction

Background

Sea freight is the most efficient method of shipping goods, achieving at least twofold lower CO_2 emissions per ton kilometre, compared to road transport by train or trucks[1]. Although fuel consumption per cargo ton-mile has improved significantly in recent decades, the simultaneous growth of freight volume has resulted in an increase of total greenhouse gas emissions. Shipping emissions cause significant harm to not only the environment via the greenhouse effect but also to human health, accounting for 250 thousand deaths and 6.4 million asthma cases annually[2]. The long-term plan for greener shipping is to achieve a 50% reduction of greenhouse gas emissions by 2050 from 2008 levels[3]. The gradually tightening Energy Efficiency Design Index (EEDI) imposes practical constraints on newbuild designs, while the recently introduced EEXI guidelines concern existing vessels. Moreover, a carbon intensity indicator (CII) has been proposed to address operational measures. The European Union has announced a plan to add shipping to the carbon trading market[4].

Efficiency gains in individual vessel components and systems, such as machinery, hull, propulsion and waste heat recovery, have been remarkable and further improvements are expected in the coming years. Nevertheless, the key changes required for reaching emissions reduction goals will be in fuel and energy conversion technology choices. The fuel of choice in shipping since the 1950s has been high sulphur residual fuel oil, converted to useful mechanical energy in a diesel engine. Low-sulphur fuels have seen increased demand since the introduction of Emission Control Areas and the global 0.5% sulphur cap has been enforced since 2020. Dual fuel engines reached the status of a mature technology over a decade ago. Due to its higher heating value compared to diesel fuels, liquified natural gas (LNG) reduces greenhouse gas emissions by 7-21%, assuming no methane leakage[5]. Although the use of fossil LNG may contribute towards short-term emissions goals, only carbon-free and synthetic fuels will provide a path to truly green shipping.

Long term shipping emissions reduction goals will be likely achieved by a mix of energy sources, carriers, and converters. Designers need to manage trade-offs in energy density, specific energy, cost and storage type when planning adoption of alternative fuels. Moreover, regulations, fuel infrastructure and converter technology will undergo a transformation during a new vessel's 25–30-year lifetime. The range of suitable retrofit technologies for a given vessel, and their economics, depend on key decisions made in the newbuild concept design phase. Failure to manage and adapt to these changes risks rendering a vessel economically unfit.

[1]Department of Mechanical Engineering, Aalto University

Corresponding author:

Antti Ritari, Aalto University School of Engineering, Department of Mechanical Engineering, Otakaari 4, Espoo, Finland.

Email: antti.ritari@aalto.fi

Related work

Assessments of means to reduce shipping greenhouse gas emissions range from global maritime transport[6] to fleets[7] and individual vessels[8–10]. The options are typically categorized as either alternative fuels or efficiency measures. Measures with high expected potential are speed reduction, wind assistance, hull coating and waste heat recovery[7]. These high-impact measures are net-present-value positive for shipowners in most scenarios, indicating that a significant amount of emissions can be reduced profitably[7]. Combining four or five high-impact efficiency measures and the adoption of LNG achieves a 50 % reduction of greenhouse gas emissions on a per vessel basis[5].

Cost-optimal selection of fuels, machinery and energy efficiency measures for a vessel involves searching through a large space of alternatives. The quality of the solutions found can be poor when derived heuristically or according to legacy design rules. Exhaustive enumeration of all alternatives is impractical due to the combinatorial nature of the problem. There are also significant interaction effects between measures[7].

Mathematical programming has received increasing attention as a tool for systematic exploration of design space in vessel powerplant design problems. Solem et al.[11] develop an integer programming model for selecting engine types and sizes for diesel electric machinery system with a tax on NO_x emissions. Baldi et al.[8] formulate a mixed-integer linear programming (MILP) model that incorporates a superstructure of alternative energy system configurations as a directed graph. The optimal configuration is extracted from this superstructure, subject to a constraint on CO_2 emissions, but retrofits are excluded. Winebreake et al.[12] present a nonlinear programming model for selecting SO_x controls for a fleet of coastal ferries.

Mathematical programming problem formulations have concentrated on the newbuild design, with some works recently also considering environmental constraints. However, models for supporting lifetime investment planning have received less attention. Balland et al.[13] address investment timing regarding energy efficiency measures under CO_2, NO_x and SO_x regulations, but this work does not discuss cost-optimal pathways to zero emissions and discards alternative fuels, fuel cells, and modification of engines.

The same authors extend the integer programming problem to machinery selection in[14]. Dual-fuel engines are selected to first run on LNG and later retrofitted to run on ammonia. Recently, Lagemann et al.[15] presented another integer programming problem formulation for vessel lifetime investment planning, considering pathway to zero and including machinery retrofits as decisions. However, the integer programming problem can only model complete energy system overhauls at predefined time slots. All continuous decision are excluded including converter sizes, tank capacities, variable lifetime of components (e.g. fuel cell system and stack) and gradual increase of battery capacity over time.

In the marine vessel design literature, the topic of lifetime planning is related to *design for modularity*. In particular, the notion of modularity in operation refers to modularity as an enabler for increasing flexibility in handling uncertainty in technical developments, and changes in operation profiles and environmental regulations[16]. In this context, Choi et al.[17] introduce a modular vessel platform consisting of slots and associated modules. The authors develop an optimization model for selecting these modules for a set of operating scenarios. However, flexibility with respect to emissions abatement scenarios is not discussed.

Aim and contribution

The authors of the present paper identify an opportunity to extend the state-of-the-art optimization-based lifetime investment planning decision models with continuous decisions corresponding to component sizes and installation periods. In particular, the current practice of discrete decision modeling of only complete system overhauls at predefined time slots, typically separated by 5–10 years, is a serious limitation when planning Li-ion battery installations for short sea vessels. The share of electricity as an energy carrier is expected to gradually increase as the cost of batteries decreases and emissions regulations strengthen, calling for high resolution modeling of installation periods and continuous modeling of component sizes.

This paper presents a multiperiod decision model for optimal selection of onboard energy system configuration under tightening CO_2 emission regulations and cost forecasts over a multidecade planning horizon. The model considers the choice of newbuild system, timing of retrofits, size and capacity of components, and allocation of fuels to converters with the objective of minimizing total cost of ownership (TCO).

The main contributions are the following:

1. A general and flexible network representation of vessel energy system that allows easily adding functions without changing the optimization problem formulation itself.
2. Decoupling of physical components (e.g., engine) and operations (e.g., combustion of fuel type) as entities allow for modeling of multipurpose converters.
3. Simultaneous consideration of discrete (installation) and continuous (sizing) design decisions in the context of vessel lifetime investment planning.
4. Modeling component installation period as a decision constrained by maximum lifetime.

Problem description and modeling approach

Network representation of onboard energy conversion systems

The problem concerns the choice of newbuild architecture, timing of retrofits, size and capacity of components, and allocation of fuels to converters with the objective to minimize TCO. As both volume and weight are constrained in marine vessels, a component may need to be replaced before reaching the end of its useful life. The problem is further complicated if the energy system modifications require extended docking of the vessel. Dockings typically take place every five years for merchant vessels[7]. However, enforcing such fixed intervals might exclude optimal installation times.

The algorithmic design approach in this work requires an explicit mathematical representation of a set of architectures

among which the vessel system is selected. Each alternative conversion path from fuel to final propulsion and hotel electrical energy demand must be unambiguously included. More specifically, the vessel energy system model must incorporate the following features:

- Conversion tasks with multiple inputs with predefined ratios (e.g., dual-fuel engine gas and pilot fuel).
- Conversion tasks with multiple outputs with predefined ratios (e.g., exhaust gas components).
- Shared material between multiple conversion tasks (e.g., a fuel type can be used in different types of converters).
- Production of the same resource by multiple conversion processes (e.g., CO_2 from combustion).
- Cross-domain energy conversions.

Mathematical representations of energy conversion and production systems take the form of a directed graph. Basic flowsheet representation uses uniform node types for representation of sequential processing steps with single inputs and outputs. Flowsheets for vessel processes have been presented in[8] and[18]. However, the uniform nodes in a flowsheet cannot represent unambiguously complex processes.

A state-task network formulation, introduced by Kondili et al.[19] and extended by Pandelides[20], is a network structure that overcomes the limitations of flowsheets. This network is a directed graph with two types of distinctive nodes: states and tasks. The state nodes represent material or energy utility resources, which are transformed by tasks. A task receives a resource from its input state in fixed proportion to its load and produces a resource to output states in fixed proportions. In this work, the energy system superstructure is modeled as a directed graph assembled from state and task nodes, due to the compact and flexible representation obtained and the generalized form that allows adding functions to the model without changing the model itself.

Figure 1 presents an illustrative example of a network representing a simplified dual-fuel engine. The states for marine diesel oil (MDO) fuel and LNG have tank storage capacity associated with them. The node PROP represents propulsion power utility which has a fixed external demand. The sum of output flows from combustion task nodes MDO-ICE and LNG-ICE must equal the external demand of PROP node. NOX is an intermediate node for NO_x present in the exhaust gas of the engine. In this node, the input flow equals the output flow. EGN represents NO_x exiting the vessel to the ambient air.

The MDO-ICE transforms the input from the MDO state to outputs to states PROP and NOX. The proportions of inputs and outputs are designated next to the network edges. In this case, one unit of output to PROP consumes 2.07 units of input MDO. Thus, the engine converts the chemical energy of the fuel to useful mechanical power with an efficiency of $1/2.07 \approx 0.483 = 48.3\%$. The task LNG-ICE consumes two inputs: LNG for primary fuel and MDO for pilot fuel. The only output is mechanical propulsion utility. Task N-CLN is the removal of NO_x from the exhaust gas.

Processing units associated with tasks are shown either directly above the task, as with a selective catalytic reduction (SCR) unit and N-CLN, or as a grey bounding box in the case

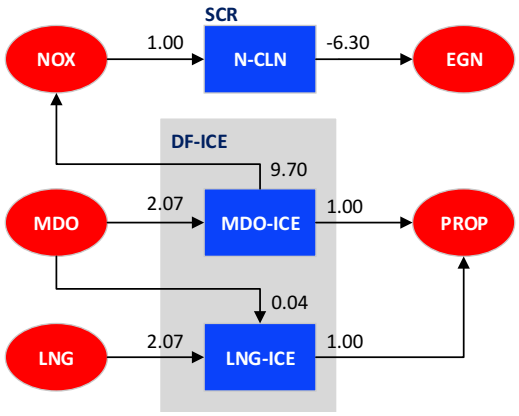

Figure 1. Network representation of vessel processes.

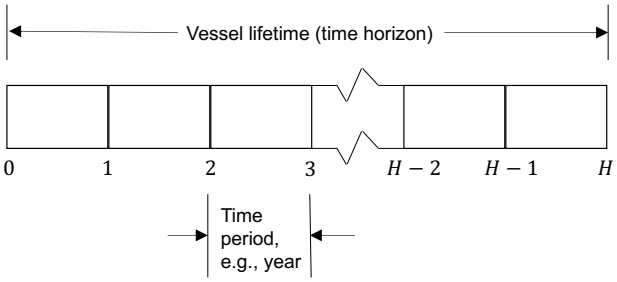

Figure 2. Discrete time representation of vessel lifetime.

that multiple tasks can be run in the same unit. Both fuel combustion tasks MDO-ICE and LNG-ICE are compatible with the dual-fuel engine unit (DF-ICE).

Time representation and investment planning modeling

Components installations take place in a time horizon that spans from newbuild phase to decommissioning of the vessel. Both continuous and discrete time representations are used in linear programming scheduling and planning models[21]. Discrete time modeling approach divides the time horizon into intervals with a uniform duration. This approach has been applied extensively in the operations research literature since introduced for the classical jobshop scheduling problem[22,23].

Discrete time models have lower complexity and computation burden compared to continuous time models. On the other hand, discretization of time may lead to sub-optimal solutions if the optimal installation times don't match with the boundaries of the interval, where installations can only take place. In this work, the discrete time representation is adopted. Discretizing the vessel lifetime to periods of one year duration is deemed reasonable and sufficiently accurate. Figure 2 illustrates the discrete time representation.

Volume constraints

The volume for onboard energy system components is limited and should be minimized to free space for revenue earning cargo and passenger spaces. In a conventional roll-on/roll-off passenger ferry with mechanical propulsion, the machinery space is located below the ro-ro decks and divided to subspaces by bulkheads. The bottom dashed rectangle

indicates machinery space and the top left rectangle at the stern indicates optional tank space in Figure 3. The four main engines (red) and four generating sets (blue) reserve approximately the same space as the MDO (green) and heavy fuel oil (HFO) (yellow) tanks (Figure 4). Recently introduced LNG fuelled ferries have deviated from the conventional design and located the LNG tank in an open area above the stern ro-ro ramp (Figure 3).

Volume as a design constraint is emphasized for alternative fuels and electrical energy storages that have lower volumetric energy densities compared to conventional hydrocarbon fuels. Horvath et al.[24] propose calculating annual revenue lost to fuel tank space, based on cargo volume displaced by fuel. The authors apply the historical average price of shipping a container. Similar values could be in principle calculated for lost cargo space in the ro-ro decks, but not for the top deck that is primarily reserved for passenger accommodation. This work assumes that the spaces in the ro-ro deck, top deck nor space above the stern ro-ro ramp are available for tanks.

Mathematical formulation of the optimization problem

The selection of units from the network superstructure, allocation of units to time slots and allocation of tasks to units involve discrete decisions. The resulting optimization problem is then combinatorial and scales exponentially in the worst case as the problem size increases. MILP is the most widely applied method for combinatorial optimization problems[21]. The solver codes for MILP allow elimination of large parts of the search space, which reduces computational burden by removing the need to exhaustively enumerate all the combinations of discrete choices. The assumption of linear relationship between variables is acceptable, as detailed nonlinear component models are not needed for investment planning.

The network structure is defined by the indexing sets $S_i, \overline{S_i}, T_s$ and $\overline{T_s}$. They define the state nodes, task nodes and their interconnections. Sets I_j and L_s map units and storages to the tasks and states, respectively. Table 1 gives the complete list of indices, sets, variables and parameters used in the mathematical model.

Constraints

State resource balance equation expresses that the amount of resource in a state s at period t is the difference between sum of inflows and sum of outflows:

$$x^S_{s,t} + \sum_{i\in T_s}\sum_{j\in K_i} \rho_{i,s} x^B_{i,j,t}$$

$$= \sum_{i\in \overline{T}_s}\sum_{j\in K_i} \overline{\rho}_{i,s} x^B_{i,j,t} + \theta_{s,t} \quad \forall s, \forall t, \tag{1}$$

where $x^S_{s,t}$ is resource consumption, $x^B_{i,j,t}$ is task load, $\rho_{i,s}$ ($\overline{\rho}_{i,s}$) is the multiplier of load for input (output) flow and $\theta_{s,t}$ is resource demand.

Constraints (2) and (3) define task execution in units. They ensure that a task can be performed in a unit only if the unit is installed. The number of tasks that are executed concurrently at a unit is constrained by Λ_j, the maximum number of tasks associated with the unit:

$$\sum_{i\in I_j} y^W_{i,j,t} \le \Lambda_j y_{j,t} \quad \forall j, \forall t, \tag{2}$$

$$y^W_{i,j,t} X^{\mathrm{B,min}}_{i,j,t} \le x^B_{i,j,t} \le y^W_{i,j,t} X^{\mathrm{B,max}}_{i,j,t} \quad \forall s, \forall t, \tag{3}$$

where $y^W_{i,j,t}$ is task status and $y_{a,t}$ is unit installation status.

The parameter V_t relates the sum of loads of all tasks run concurrently in unit j at period t to the size x^P_j and installation status of the unit:

$$\sum_{i\in I_j} \frac{x^B_{i,j,t}}{V_t} \le x^P_j y_{j,t} \quad \forall j, \forall t. \tag{4}$$

A subset of states require storage capacity. The set L_s denotes storages capable of storing material resource for state s. The initial stock of resource at a state, at each period, cannot exceed the installed capacities of all storages dedicated to the state. Moreover, the storage must be installed at the period t for the storage capacity to be accessible:

$$x^S_{s,t} \le \sum_{l\in L_s} y_{l,t} x^P_l \quad \forall s, \forall t. \tag{5}$$

A component is available for use from its installation until either the end of its lifetime is reached or a premature uninstallation takes place. Constraints (6) and (7) encode this functionality by the full backward propagation method[21]:

$$y_{a,t} = \sum_{t'=\max\{1,t-H\}}^{t} y^{\mathrm{in}}_{a,t'} - y^{\mathrm{out}}_{a,t'} \quad \forall a, \forall t, \tag{6}$$

$$y^{\mathrm{out}}_{a,t} \le \sum_{t'=\max\{1,t-N_a+1\}}^{t} y^{\mathrm{in}}_{a,t'} \quad \forall a, \forall t, \tag{7}$$

where $y^{in}_{a,t}$ is installation decision, $y^{\mathrm{out}}_{a,t}$ is the uninstallation decision, N_a is component lifetime and H is the number of periods. The first constraint (6) states that the binary variable $y_{a,t}$, which indicates installation status, receives a value of one at all periods that succeed installation and precede uninstallation periods. The second constraint (7) enforces uninstallation before the maximum lifetime has been exceeded.

The backward propagation requires three additional constraints. These ensure that a component can be installed and uninstalled only once, and installation decision must be always coupled by an uninstallation decision at a later period (which can be the final period, e.g. decommissioning):

$$\sum_{t=1}^{H} y^{\mathrm{in}}_{a,t} \le 1 \quad \forall a, \tag{8}$$

$$\sum_{t=1}^{H} y^{\mathrm{out}}_{a,t} \le 1 \quad \forall a, \tag{9}$$

$$\sum_{t=1}^{H} (y^{\mathrm{out}}_{a,t} - y^{\mathrm{in}}_{a,t}) = 0 \quad \forall a. \tag{10}$$

The decision to dock at the beginning of period t, denoted by the binary variable y^D_t, must be coupled with the

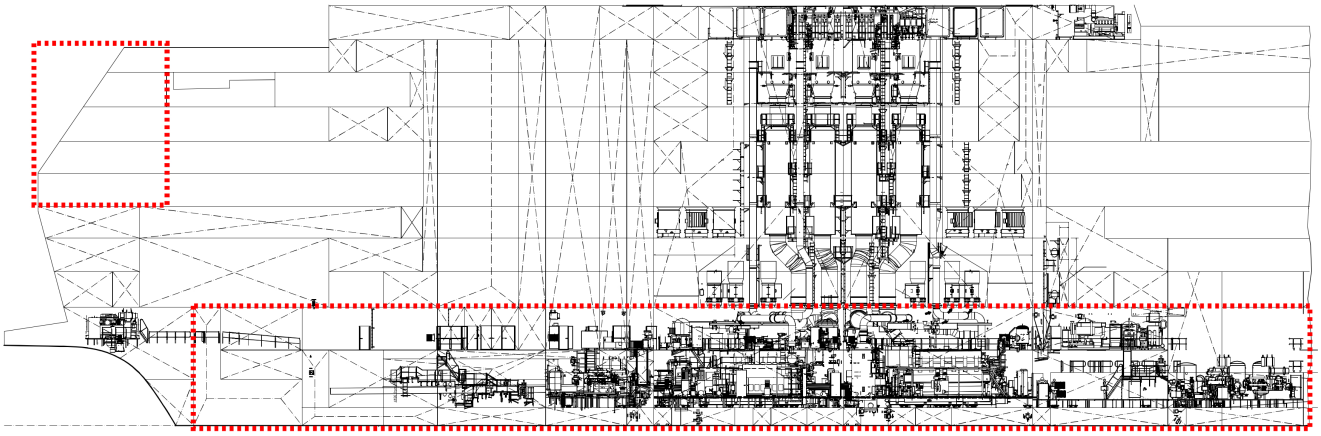

Figure 3. Side view of roll-on/roll-off passenger ferry aft general arrangement.

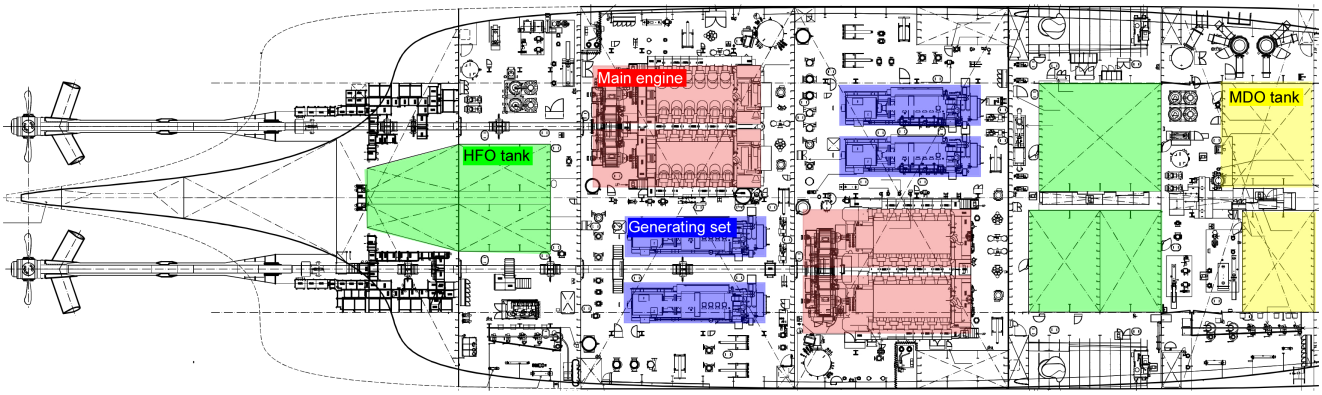

Figure 4. Top view of roll-on/roll-off passenger ferry machinery space general arrangement.

Table 1. Model notation.

Symbol	Description	Symbol	Description
Indices		*Parameters*	
i	Task	$\rho_{i,s}$	Proportion of input of task i from state $s \in S_i$
j	Unit	$\overline{\rho}_{i,s}$	Proportion of output of task i to state $s \in \overline{S_i}$
s	State	$X_{i,j}^{\text{B,max}}$	Maximum capacity of unit
l	Storage	$X_{i,j}^{\text{B,min}}$	Minimum capacity of unit
a	Component (unit or storage)	Ω	Maximum number of lifetime dockings
		H	Time horizon (vessel lifetime)
Indexing sets		N_a	Maximum lifetime of component a
S_i	States which feed task i	M	Number of voyages annually
$\overline{S}_i$	States which task i produces as outputs	$\theta_{s,t}$	External demand for resource of state s at period t
K_i	Units capable of performing task i	V_t	Duration of a characteristic voyage at period t
T_s	Tasks receiving resource from state s	P_t^{CO2}	CO_2 limit at period t
$\overline{T}_s$	Tasks producing resource in state s	F_a	Specific floor area of component a
I_j	Tasks which can be executed by unit j	F^{MAX}	Floor area of machinery space
L_s	Storages for resource in state s	C_t^{CO2}	Cost of emitting one ton of CO_2
		C_a	Fixed cost of component a
Continuous variables		C_a, t^{var}	Variable cost of component a at period t
$x_{i,j,t}^{B}$	Load of task i in unit j at period t	C_s, t^{B}	Cost of consuming state s at period t
$x_{s,t}^{S}$	Consumption of resource in state s at period t	Λ_j	Maximum number of tasks that can run concurrently in unit j
x_j^{P}	Installed size of component a		
Binary variables			
$y_{i,j,t}^{W}$	Task i runs in unit j at period t		
$y_{a,t}$	Installation status of component a at period t		
$y_{a,t}^{\text{in}}$	Decision to install component a at period t		
$y_{a,t}^{\text{out}}$	Decision to uninstall component a at period t		
y_t^{D}	Decision to dock at the beginning of period t		

installation decisions of a component:

$$y^{\text{in}}_{a,t} + y^{\text{out}}_{a,t} \leq 2y^{D}_{t} \quad \forall a, \forall t, \tag{11}$$

$$\sum_{t=1}^{H} y^{D}_{t} \leq \Omega, \tag{12}$$

where Ω is the maximum number of allowed dockings during the vessel's lifetime.

The constraint for CO_2 emission limit states that total inflow of material to the state CO_2 must not exceed the limit for each period:

$$x^{S}_{\text{CO2,t}} \leq P^{\text{CO2}}_{t} \quad \forall t. \tag{13}$$

The available floor area for component installation is constrained by the machinery space area F^{MAX}:

$$\sum_{a} x^{P}_{a} y_{a,t} F_{a} \leq F^{\text{MAX}} \quad \forall t, \tag{14}$$

where F_a is the specific floor area of component a.

Objective function

The objective function to be minimized is the TCO:

$$f_{obj} = \sum_{t=1}^{H} \left[C^{\text{CO2}}_{t} x^{S}_{\text{CO2,t}} + \sum_{s} C_{s,t} x^{S}_{s,t} + \frac{1}{M} \sum_{a} (C_{a} y^{\text{in}}_{a,t} + C^{\text{var}}_{a,t} x^{P}_{a} y^{\text{in}}_{a,t}) \right], \tag{15}$$

where the cost parameters are C^{CO2}_{t} for CO_2 emissions, $C_{s,t}$ for resource consumption, C_a for fixed unit installation and C_a, t^{var} for unit size. Finally, M is the number of annual voyages.

The elements of TCO are installation capital expenditures and the operation costs, which are comprised of fuels and shore electricity in the case that the vessel is equipped with a battery. The capital costs are accounted for on a voyage basis by dividing them with the number of annual voyages. Costs that are the same between all the alternatives configurations are neglected, because they don't influence the optimal solution.

Lossless linearization of nonlinear constraints

Constraint (5) features a nonlinear and nonconvex expression of a product of two decision variables, which is not compatible with the a linear programming problem formulation. However, since the first variable is binary and the second is continous and nonnegative, a lossless linearization technique is applicable[25]. Constraint (5) is reformulated by substituting the bilinear term $y_{l,t} x^{P}_{l}$ with a new nonnegative continuous variable x^{aux}_{l}:

$$x^{S}_{s,t} \leq \sum_{l \in L_s} x^{\text{aux}}_{l} \quad \forall s, \forall t. \tag{16}$$

In addition, three new linear constraints are needed to ensure equivalence to the original nonlinear constraint:

$$x^{\text{aux}}_{l} \leq u_{l} y_{l,t} \quad \forall l, \forall t, \tag{17}$$

$$x^{\text{aux}}_{l} \leq x^{P}_{l} \quad \forall l, \forall t, \tag{18}$$

$$x^{\text{aux}}_{l} \leq x^{P}_{l} - u_{l}(1 - y_{l,t}) \quad \forall l, \forall t, \tag{19}$$

where u_l is a tight upper bound on x^{P}_{l}. All the other nonlinear terms are linearized accordingly.

Implementation

The optimization problem presented in the previous section was implemented using Python interface of the commercial software Gurobi. Problem instances were solved with Gurobi 9.1 with the default settings. The solution times for the problem instances ranged from seconds to a few minutes. Further reporting of solution times is omitted from the sections that follow.

Alternative energy conversion pathways and component choices

This section presents an overview of alternative fuels and onboard energy conversion architectures that enable the transition to zero emissions. Focus is on the basic properties of fuels and required onboard components, instead of onshore infrastructure.

Fuels

As the cleanest fossil fuel, natural gas generates the least CO_2 per unit of useful energy output and adoption LNG in shipping reduces CO_2 emissions per ton-km. Natural gas derived from biomass (biomethanol) can achieve close to net zero CO_2 emissions and it can be mixed to fossil sources by different ratios (Figure 5). Exponentially increasing installed capacity, and reducing cost, of wind turbines and photovoltaic cells is giving rise to an adoption of fuels produced using green electricity. Hydrogen production by electrolysis requires only water and electricity. Ocean crossing vessels store the hydrogen onboard as a liquid at cryogenic temperature -253 C. In addition to the complexity arising from cryogenic storage, the tank volume is more than twofold for storing a given amount of energy in hydrogen compared to LNG[8].

Synthetic hydrocarbon fuels are derived by bounding hydrogen to carbon. These fuels can achieve CO_2 neutrality since the same amount of CO_2 emitted in combustion has been extracted from air (or from industrial process before exhaustion) during production. An alternative pathway from hydrogen to a liquid fuel in ambient conditions is the Haber-Bosch process, which does not involve carbon, but instead bounds hydrogen to nitrogen to produce ammonia.

Electrical energy storage

Lithium-ion battery systems have increased in size and production volume in recent years due to fast market adoption of fully electric passenger vehicles. The losses from charging and discharging a battery are negligible compared to electrolysis and hydrogen-to-electricity conversion. On the other hand, the volumetric energy density of high-energy lithium-ion battery systems is less than one tenth of liquid hydrogen[27]. This property renders batteries infeasible for storing all the energy needed to propel a deep sea vessel on an ocean crossing voyage. However, short sea vessels are promising candidates for hybrid power sources that contribute to propulsion in combination with other use cases such as safety reserve power[28].

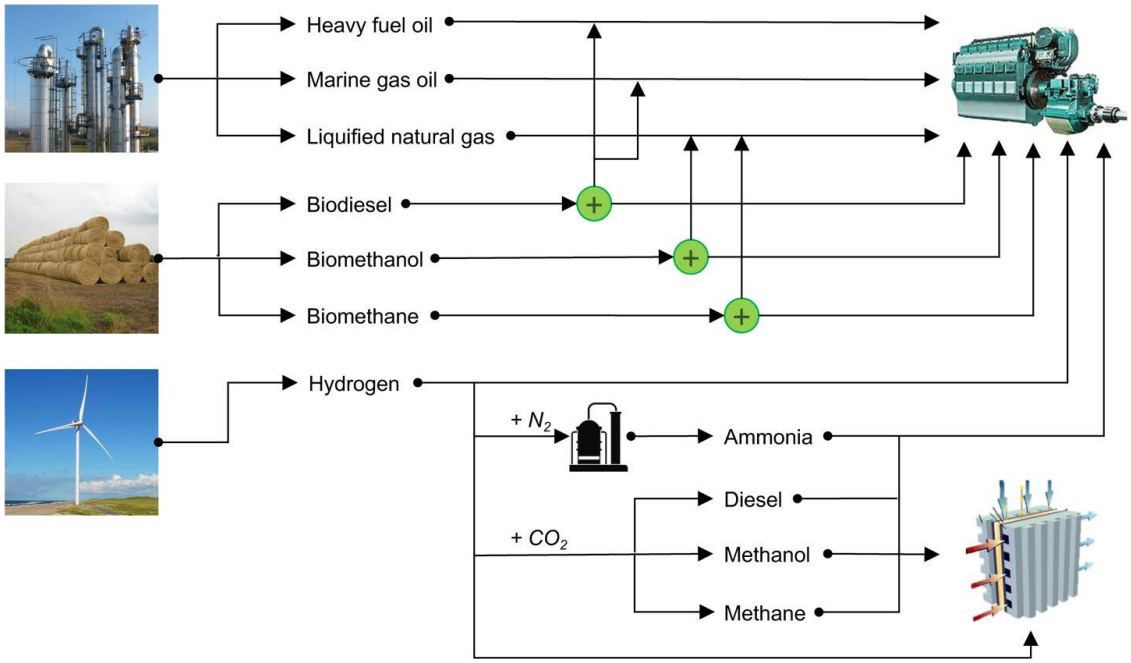

Figure 5. Future fuels. Adapted from[26]. Images are from Wikimedia.

Converters

The conventional prime mover, internal combustion engine, can be converted to run on any liquid or gaseous fuel featured in Figure 5. Recent research and development efforts by marine engine manufacturers have focused on converting four stroke engines to run on 100% hydrogen[29].

Fuel cells convert the chemical energy of fuels to electricity by oxidation and reduction reactions. Since fuel cells are not heat engines, they are not bounded by the same thermodynamic constraints, e.g. Carnot's law[18], which allows higher conversion efficiency. Proton exchange membrane (PEMFC) and solid oxide fuel cells (SOFC) have been identified the most promising for shipping applications[30]. PEMFC only runs on pure hydrogen, whereas the high temperature of SOFC allows ammonia and hydrocarbon fuel use.

Numerical examples

Case vessel characteristics

Data acquired from a Baltic Sea roll-on/roll-off passenger ferry defines voyage energy and power requirements for all the numerical example problems. The vessel is equipped with a conventional direct driven mechanical propulsion, with four medium speed diesel engines that drive two main propeller shafts via reduction gearboxes. Technical data of the vessel is given in Table 2.

The vessel operates in a 48-hour cycle (Figure 6) on a route between Helsinki, Finland and Stockholm, Sweden. Speed profile is composed of mainly open sea cruising at 18 knots (Figure 7). Figure 7 shows the propulsion power and cumulative energy consumption, while Table 3 breaks down

Table 2. Data for the case vessel.

Parameter	Unit	Value
Length overall	m	203
Gross tonnage	gt	58,376
Design speed	kn	23
Rated main engine power	kW	4×8,145
Average hotel power	kW	1500
Machinery space area	m^2	300

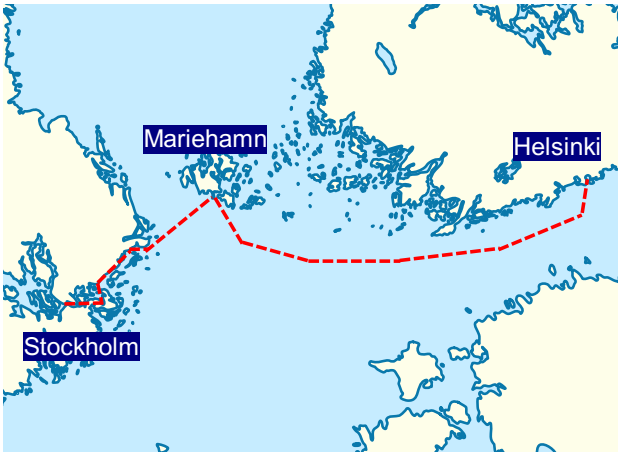

Figure 6. Case vessel route in the Baltic Sea.

the consumption by voyage legs. The propulsion energy consumption is approximately 195 MWh on the sailing legs between Helsinki and Stockholm. The visit in Mariehamn is brief and does not allow bunkering or battery charging. On the other hand, both Helsinki and Stockholm ports are equipped with high voltage onshore power supply. Since the

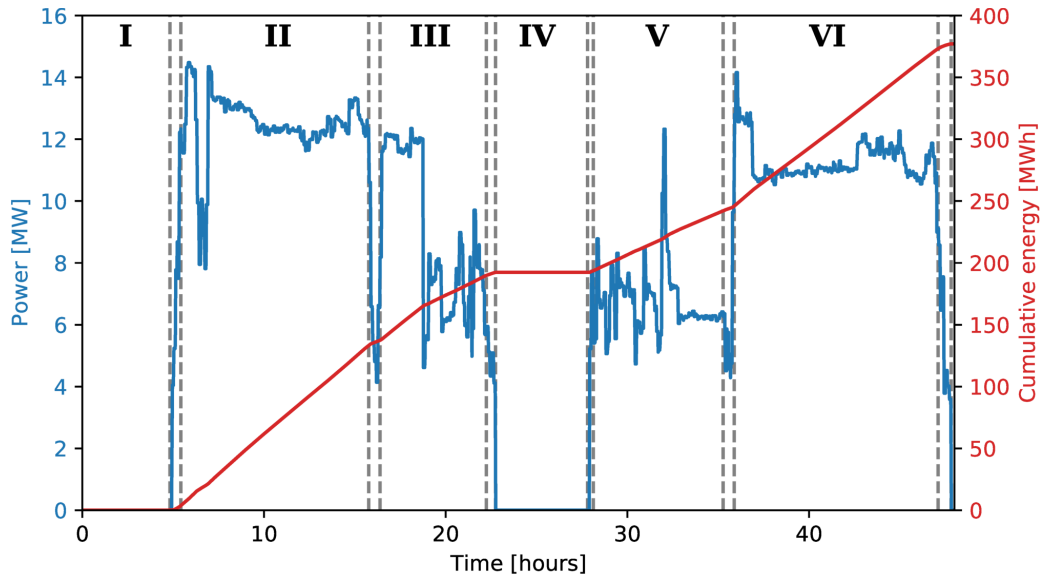

Figure 7. Reference operational profile (propulsion power vs. time) of the case vessel. The roman numerals indicate the main sailing legs and stops in ports of Helsinki, Finland and Stockholm, Sweden.

IEEE 80005 2.5 MW 11 kV/50 Hz standard is not designed for high capacity battery system charging, it is not considered a constraint in the example problems.

Table 3. Characteristic roundtrip voyage propulsion energy demand by sailing leg.

Leg	Description	Energy [MWh]
I	Moored in Helsinki	0
II	Helsinki - Mariehamn	130
III	Mariehamn - Stockholm	60
IV	Moored in Stockholm	0
V	Stockholm - Mariehamn	55
VI	Mariehamn - Helsinki	125

Hybrid propulsion

The numerical problems assume an electric machine connected to the propeller shaft via a reduction gearbox. In this hybrid propulsion (Figure 8) configuration, the electric machine can boost the propeller in power take-in (PTI) mode, or generate electricity in power take-off (PTO) mode. PTO is the default means of electricity generation and generating sets are assumed only for reserve power. Controllable pitch propeller allows the main engine(s) and the electric machine to rotate with constant speed independent of load. Electrochemical devices connect to the main switchboard via an inverter. Since the vessel is equipped with two shaft lines, the single shaft design is duplicated as in Figure 4.

Cost data

The data input used in the problem instances is presented in Tables 4-7 for conversion units, exhaust gas cleaning devices, storages, fuels and electricity. Table 4 presents data for units based on [8,31,32] and author estimations. Size dependent (variable) costs are stated for the first and last period of the lifetime. Other values are given by linear interpolation. Fixed cost of 50k€ is assigned to the installation of all units except fuel cell stacks.

HFO, MDO and LNG prices presented in Table 7 are estimates obtained from historical prices in the Port of Rotterdam [33]. While there is large variation and uncertainty in development of prices in absolute terms, the relative prices between fuels determine the decisions regarding fuel choices. The absolute price effects comparisons to unit capital cost. Prices for E-fuels are based on the lower bound price scenario in [34] via [15].

Emission factors

Generation of electricity drawn from the grid to onshore power supply and fuel production is assumed 100% renewable. Only electricity pathway for hydrogen, methanol and ammonia production is included. In the green hydrogen production pathway for hydrocarbon fuels, CO_2 is captured from air or from an industrial process. The tank to propeller (downstream) CO_2 emissions are cancelled out by the captured CO_2, and as a results the net well-to-tank CO_2 emission are zero. Well-to-tank and tank-to-propeller emission factors for fossil fuels reported in Table 4 are from [8].

Superstructure configuration

The superstructure of alternative vessel energy system configurations and operation modes is represented as a state-task network. Since the solver algorithm cannot generate solutions outside of the alternatives considered in the network, it must exhibit all the alternatives. Figure 9 shows the network applied in all problem instances. Table 4 gives the units compatible with each task and Table 6 gives storages associated with the a subset of states.

The set of alternative energy converters consists of medium speed diesel engine (ICE), DF-ICE, PEMFC and SOFC. PEMFC converts pure hydrogen (H2) only, while SOFC runs on LNG, synthetic liquified natural gas (eLNG), methanol (MTH) and ammonia (NH3). Hydrogen is bunkered to pressurized or cryogenic tanks. Production of hydrogen from ammonia by cracking is excluded. The

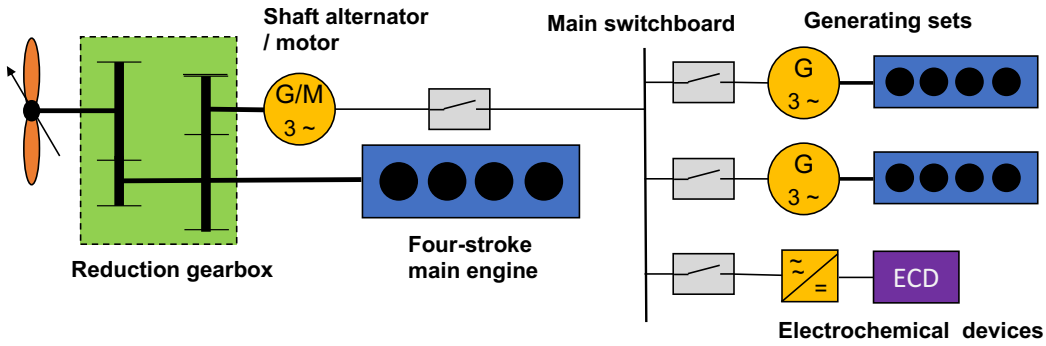

Figure 8. Layout of the mechanical propulsion configuration.

Table 4. Data for physical units associated with tasks. Abbreviation k€stands for thousand euros.

ID	Description	Lifetime [y]	Floor space [m^2/MW]	Variable cost [k€/MW]
ICE	Medium speed diesel engine	25	3.5	(240, 240)
DF-ICE	Medium speed dual fuel engine	25	3.5	(470, 470)
H2-CMB	Engine modification for hydrogen combustion	25	0.1	(200, 180)
NH3-CMB	Engine modification for ammonia combustion	25	0.1	(150, 130)
MTH-CMB	Engine modification for methane combustion	25	0.1	(150, 130)
PEMFC	Proton exchange membrane fuel cell stack	8	0.23	(275, 138)
PEM-SYS	Auxiliary components for PEMFC	25	1	(730, 365)
SOFC	Solid oxide fuel cell stack	6	0.23	(640, 320)
SO-SYS	Auxiliary components for SOFC	25	1	(1280, 640)
INV	Battery power electronics	25	1.1	(100, 100)
EM	Propeller shaft generator/motor	25	2.9	(110, 110)
SWS	Seawater scrubber	25	0.1	(375, 375)
SCR	Selective catalytic reduction system	25	0.1	(46, 46)

Table 5. Description of tasks and their mapping to units.

ID	Description	Unit(s)	Efficiency [%]
X-ICE	Combustion of fuel X ∈ {HFO, MDO, eMDO, H2, NH3, MTH} in an internal combustion engine	ICE, DF-ICE	45
X-ICE	Combustion of fuel X ∈ {LNG, eLNG}	DF-ICE	45
X-RF	Feeding of fuel X ∈ {H2, NH3, MTH} to engine	X-CMB	100
X-SO	Electrochemical conversion of fuel X ∈ {LNG, eLNG, H2, NH3, MTH} to electricity in a solid oxide fuel cell	SOFC	55
SO-AUX	Auxiliary tasks of a solid oxide fuel cell	SO-SYS	100
H2-PEM	Electrochemical conversion of hydrogen to electricity in a proton exchange membrane fuel cell	PEMFC	55
PEM-AUX	Auxiliary functions of a proton exchange membrane fuel cell	PEM-SYS	100
DISC	Battery discharge to the grid	INV	97
PTO	Shaft electric machine in generator mode	EM	97
PTI	Shaft electric machine in motor mode	EM	97
S-CLN	Removal of SO_x from exhaust gas	SWS	-
N-CLN	Removal of NO_x from exhaust gas	SCR	-

mechanical and electrical resources in PROP and auxiliary electricity grid (GRID) nodes, respectively, are consumed externally.

While the conversion of chemical energy in MDO, HFO and LNG to useful mechanical energy requires only one task, hydrogen conversion in an engine involves two consecutive tasks: feed of hydrogen to the engine (H2-RF) and combustion (H2-ICE). Here the task H2-RF is associated with the unit H2-CMB, which is the modification of a conventional diesel engine for combustion of 100% hydrogen. Thus, task H2-ICE is blocked unless the unit H2-CMB is installed. The same logic applies to methanol and ammonia conversion in engines.

Problem instance definitions

This section presents four numerical example problems, labelled P1 to P4. All the problems share the network superstructure of alternative designs (Figure 9) and the data in Tables 4-7. Both shaft lines of the case vessel twin-screw design are assumed identical. The voyage power and energy requirements (Figure 7) are divided evenly between the shaft lines. All the problem formulations and solutions are reported for a single shaft line.

While CO_2 emission regulations are problem instance specific, NO_x and SO_x regulations are uniform. Tier III regulations are enforced for NO_x and Emission Control Area limit for SO_x.

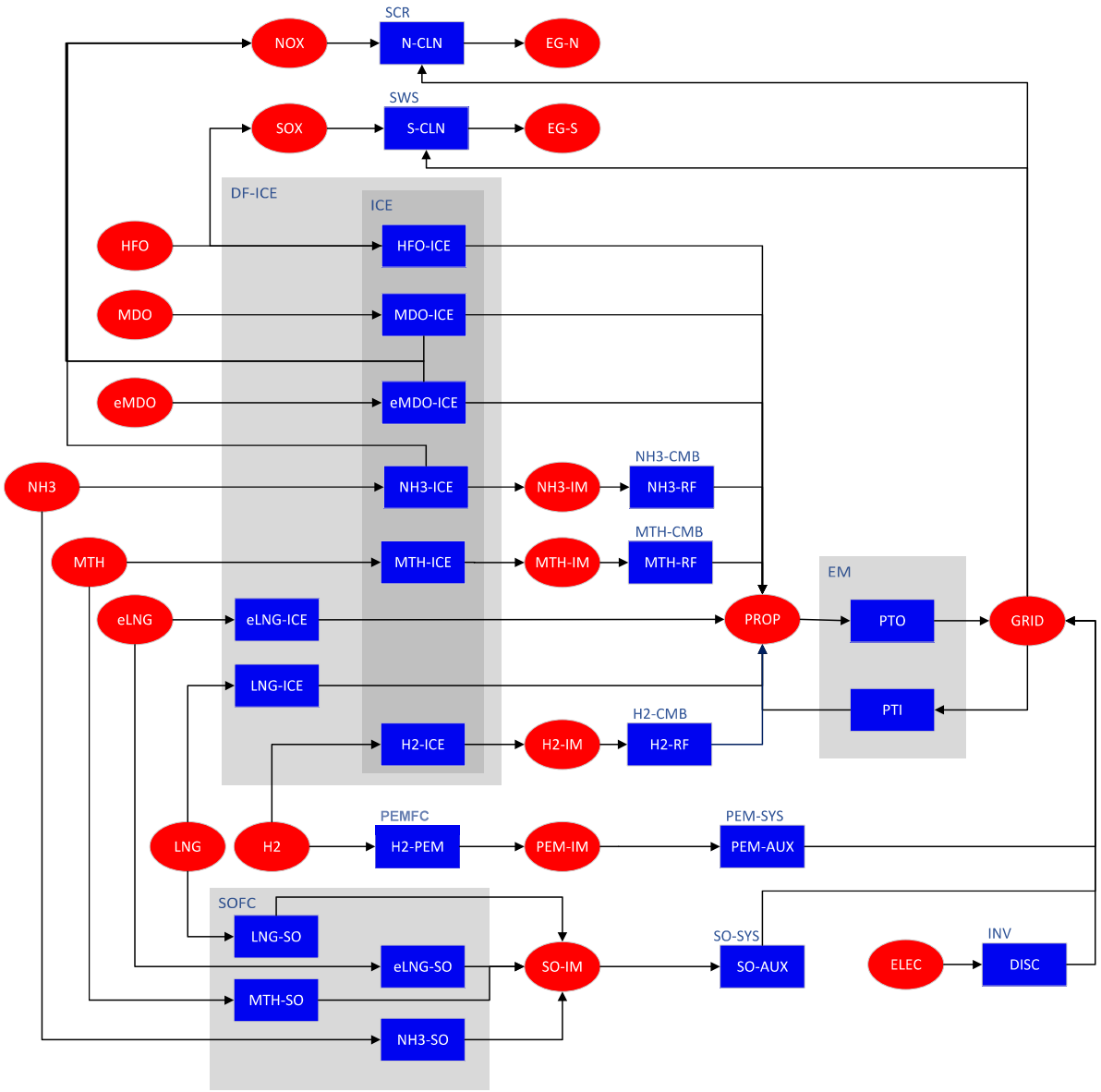

Figure 9. Superstructure of the energy system represented as a network of state nodes (red) and task nodes (blue). The abbreviations above the task nodes point to the units that run the corresponding task. See Tables 7, 4 and 5 for descriptions of the nodes and units.

Table 6. Data for energy storage units. Costs are given for the first and last period of the lifetime. Other values are linearly interpolated. The floor areas can be calculated from the reported volumes by applying a fixed tank height set by the machinery space height. Volumes are author estimations.

ID	Energy carriers	Lifetime [y]	Volume [m^3/MWh]	Cost [k€/MWh]
HFOL	HFO	25	0.1	(0.08,0.8)
MDOL	MDO, eMDO	25	0.1	(0.1,0.1)
LNGL	LNG, eLNG	25	0.16	(0.31,0.31)
NH3L	NH3	25	0.28	(0.15,0.15)
MTHL	MTH	25	0.23	(0.14,0.14)
H2L	H2 (liquid)	25	0.4	(0.8,0.7)
H2G	H2 (gas)	25	1.6	(0.4,0.35)
BTR	ELEC	10	11.3	(300,100)

Table 7. Data for fuels. The IDs denote the states associated with fuels in the network representation. The prefix *E* stands for electro-fuel, WTT for well-to-tank and TTP for tank-to-propeller. Prices are stated for the first and last period of the lifetime. Other values are given by linear interpolation.

ID	Description	WTT CO_2 [kg/MWh]	TTP CO_2 [kg/MWh]	Price [€/MWh]
HFO	HFO	0	291	(30,30)
MDO	MDO	0	290	(50,50)
eMDO	E-MDO	-290	290	(450,333)
LNG	LNG	0	200	(60,60)
eLNG	E-LNG	-200	200	(230,170)
H2	E-hydrogen	0	0	(170,120)
NH3	E-ammonia	0	0	(180,130)
MTH	E-methanol	-262	262	(280,210)

P1: Fixed dual-fuel engine configuration. This is a baseline scenario that considers a fixed dual-fuel engine configuration for the entire vessel lifetime. The only decision is the fuel mix, which is limited to some combination of HFO, MDO, LNG, synthetic marine diesel oil (eMDO) and eLNG. A strict linearly decreasing CO_2 emission

constraint is enforced. The initial limit follows current EEDI regulations, and the final limit is zero, i.e. emission free.

P2: CO_2 limit with flexible configuration. The same gradually tightening CO_2 limit as in P1 is enforced, but all the artificial limitations on the energy system design and operation, both for newbuild and retrofits, are relaxed. In this case all the alternative units, tanks and fuels defined in the superstructure (Figure 9) are available.

P3: CO_2 limit with batteries excluded. The problem equals P2 with the exception that batteries are excluded from the available storage units. This problem instance is motivated by limited mooring time and onshore power supply availability that many short sea vessels are subjected to.

P4: CO_2 pricing with flexible configuration. Fully flexible configuration as in P2 and P3 is allowed, but a price on emitted CO_2 is applied instead of a strict limit as P1 to P3. The price increases linearly from zero to 200 €/tonCO_2.

Results

Optimal solutions of P1 to P4 are visualized in Figures 10 to 13. Each figure features top and bottom elements. The top element is a bar chart that illustrates component installation periods over the lifetime of the vessel. The blue bars are converter units and the green bars are storages. The bottom element of the figure shows the contribution of fuel types and electricity to the total demand.

Task loads are shown explicitly for the solution of P1 in Figure 10. The task loads of problems P2 to P4 are not shown, but they can be inferred from the component installation and fuel use plans. For example, consider the operation of the shaft electric machine that is associated with PTO and PTI tasks. In the solution of P4 (Figure 11), the electric machine runs in PTO mode in years one and two, because this is the only electricity generation path when batteries or fuel cells are not installed. On the other hand, from the year three onwards the first installed battery discharge exceeds 25 MWh during a voyage, but the hotel load is only 18 MWh. The difference is provided to propeller via the electric machine in PTI mode.

Solution P1: CO_2 limit with invariable configuration

The baseline configuration remains invariant throughout the lifetime (Figure 10, top) as expected. Full size tank for LNG is installed in the newbuilding phase and remains in use until decommissioning. Fuel switching is the only means of compliance with CO_2 limit.

The first year is operated with 100% MDO. Starting from the second year, MDO is gradually switched to LNG, which emits less CO_2, but is more expensive. Starting from year six, eLNG is introduced first in a small amount and then with increasingly larger quantities as a substitute to LNG. The shaft electric machine functions in PTO mode for the entire lifetime. It is dimensioned according to the auxiliary electricity demand and conversion losses.

SCR system is installed for cleaning NO_x emission from combustion of MDO. Scrubber is not needed, because MDO sulphur content is lower than the limit in emission control area. Small amount of MDO is still used as pilot fuel. The size of the MDO tank in MWh is slightly larger than the LNG tank. The difference is due to the fact that SCR consumes a small amount of electricity. Exhaust gas cleaning is needed only when running on MDO.

Solution P2: CO_2 limit with flexible configuration

The solution of P2 exhibits a complex pattern of installations and removals of converters and storages throughout the lifetime (Figure 11). The newbuild is equipped with two engines of different sizes, but the smaller 3.33 MW engine is removed after only five years of use. The larger engine is converted to run on hydrogen from the beginning with the installation of the unit H2-CMB.

HFO is gradually substituted by hydrogen and electricity to comply with tightening CO_2 limit. Both hydrogen and HFO are used in the engine from year eight onwards. If a specific mix of these fuels is not viable for combustion directly, the mix can be understood as fuel switching within a voyage.

First battery pack is installed at year three substituting MDO with electricity. Second battery pack is installed three years later which corresponds with the removal of the smaller diesel engine. The share of electricity saturates at 19% already by the sixth year when the second battery system is installed. The limiting factor is the machinery space, which does not have sufficient space for power electronics and battery modules required by a fully battery powered vessel. The first battery reaches its end of life by year 11 and a replacement system is installed. The second battery is removed at this time, before exhausting the full lifespan.

Solution P3: CO_2 limit with batteries excluded

In this case compliance with CO_2 limit is attained by gradually shifting from HFO to green hydrogen (Figure 12). In contrast to P2, electrical energy is not stored onboard due to the exclusion of batteries. Support for hydrogen combustion in an engine is installed already for the newbuild. For the first six years, hydrogen is only used in the engine. PEMFC is installed at the beginning of year seven. After the fuel cell installation, hydrogen consumption shifts entirely from the engine to the fuel cell until its maximum power limit is reached. After this point, the engine starts running on hydrogen again with increasing quantity until the last year when HFO has been completely phased out.

The shaft electric machine is sized according to the maximum power that the fuel cell delivers from the grid to the shaft. For the first six years, auxiliary electricity demand is supplied by the engine via PTO function. However, the required power is only approximately half of the installed power of the electric machine. Following the fuel cell system installation the electric machine power flow direction turns over. In PTI mode, the electric machine delivers power to the shaft at its maximum rating.

Solution P4: CO_2 price with flexible configuration

Solution for the carbon pricing scenario P4 (Figure 13) shows that operating with HFO and paying the CO_2 price is more attractive economically emission abatement by switching to alternative fuels. Installation of a battery system

at the end of year ten is the only retrofit modification to the vessel. The inverter is installed already in the newbuilding phase, although it has no use until year 11 when the battery system becomes online. In this case the solver is indifferent between installation times because installation cost is constant over time. To avoid tying up capital unnecessary, premature installations should be avoided in practice.

Comparison of total cost of ownership

Table 8 reports objective function values for the optimal solutions of P1 to P4. The objective to be minimized is TCO on a voyage basis. The total realized cost can be calculated by multiplying the reported TCO by the number of annual voyages N.

Table 8. Optimal TCO on voyage basis.

Problem	CO_2 rule	Configuration	TCO [k€]
P1	Limit	DF-ICE only	579.8
P2	Limit	Free	344.4
P3	Limit	Battery excluded	435.7
P4	Price	Free	313.9

Discussion

A comparison of solutions P1 and P2 illustrates the retrofit option value. On a voyage basis, the flexible configuration achieves 40.6 % lower TCO (Table 8). The improvement is attributed to the modification of engines for hydrogen combustion and the installation of batteries for storing electrical energy onboard.

Solutions to P2 and P4 feature high-energy battery installations. The combination of tightening the CO_2 limit and decreasing battery cost favors electricity as an energy carrier over synthetic fuels already in the third year. Comparing solutions P2 and P3, 21% lower TCO can be attributed to batteries. Although batteries clearly show value in this short sea shipping problem, the limited space onboard remains an issue.

The results are in line with previous work that has found green hydrogen as the optimal fuel choice for newbuild zero-emission vessels[8]. However, while PEMFC has been found optimal for a newbuild zero-emission vessel, an ICE retrofitted with hydrogen combustion modifications is favored when the lifetime evaluation scope is adopted.

Lagemann et al.[15] present a vessel energy system design method that incorporates discrete design decisions over the lifetime, i.e., complete overhauls of the energy system and fuel type at fixed intervals. The case study evaluates optimal newbuild system and retrofits for a Supramax bulk carrier over a 30-year lifetime. The optimal pathway follows from the initial dual-fuel engine and LNG design to the adoption of green hydrogen. Although the discrete modeling approach attains the same general zero emission pathway as the continuous approach in this paper, it is evident that gradual changes in fuel choice and component investment are key characteristics of the optimal solution.

Conclusions

Optimal design choices under green transition

In general, the energy system and fuel choice follow the primary energy source transition from fossil hydrocarbon fuels to green electricity. In this transition, retrofits play a key role in enabling the use of hydrogen, ammonia, or methanol. Fuel switching from LNG to eLNG alone is not economically viable. However, the optimal fuel and component choices are strongly influenced by the CO_2 regulation scheme. While a hard limit on CO_2 emissions forces the adoption of alternative fuels and energy system modifications, the optimal response to a CO_2 pricing scheme is paying the fee while sailing using conventional fossil hydrocarbon fuels.

Internal combustion engines are today the standard choice for energy conversion in newbuilds. Although fuel cells achieve higher conversion efficiency than engines, the adoption of fuel cells by the industry is likely to remain marginal for a long time due to the inertia of the large stock of engine investments. Modification of engines for support of alternative fuels is a favourable choice over retrofit of fuel cells. This also suggests that drastically costly wrong choices in the newbuild phase are unlikely given that the optimal pathway involves retrofit modifications of conventional engines anyway.

Future-proof choices

For short sea vessels, such as the roll-on/roll-off passenger ferries, batteries are expected to play an important role in the green transition. Although batteries are not the least-cost choice for newbuild short sea vessels, retrofits are included in the optimal pathway to zero emissions. The newbuild design should reserve sufficient space for high-energy battery installation and ensure compatibility with other components. The optimization framework introduced in this work provides decision support for the optimal timing of battery installations, given predictions of capital cost, electricity price, and emissions regulations. Components are occasionally removed before they have reached their end of life to free machinery space for retrofitted components such as batteries and power electronics. The optimal installation period can be remarkably short, only a few years.

The results show that, in all the optimal pathways, the power delivered by batteries and/or fuel cells increases during the lifetime. Moreover, these devices not only provide the auxiliary electricity demand, but also contribute to propulsion by delivering power from the grid to the propeller via a shaft electric machine. Hybrid propulsion, i.e., mechanical propulsion line with shaft electric machine, is the key design choice that enables retrofitted batteries to contribute to propulsion. In this context, designing newbuild hull form and machinery space with shaft electric machine and gearbox in mind, as well as its dimensioning, are of critical importance. A key question is whether to dimension an electric machine larger than required for the first years of operation, keeping in mind retrofits. Expected battery retrofits also interact with hydrogen tank choice, as storing hydrogen as liquid takes less space than pressurized gas.

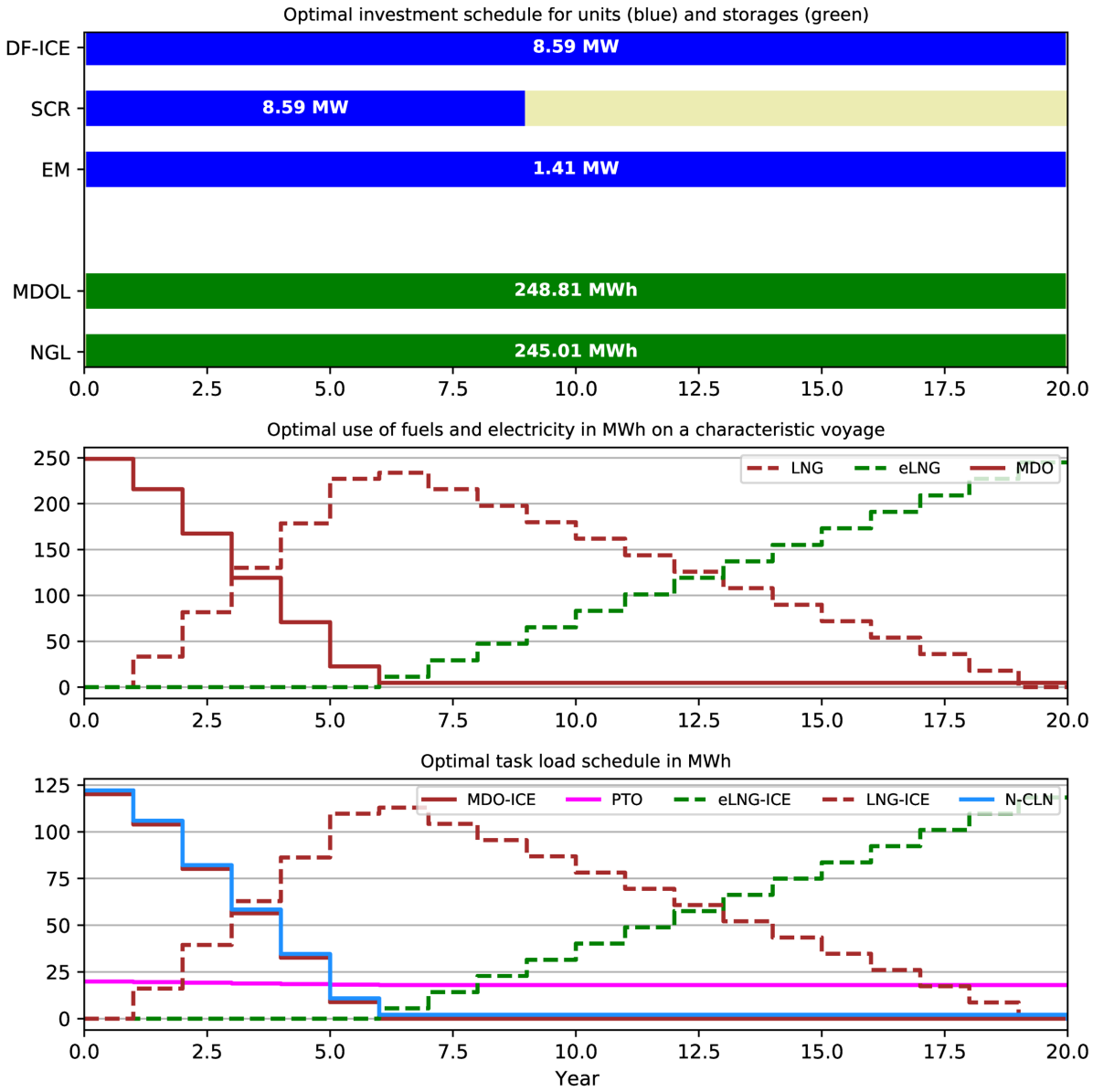

Figure 10. Optimal investment, fuel use and task schedule for the baseline scenario (P1).

Acknowledgements

The authors thank Tallink Silja Oy for providing operational data of the case study vessel in connection with Business Finland's INTENS project (ref. 8104/31/2017).

Funding

This research was funded by Business Finland's Clean Propulsion Technologies project (ref. 38485/31/2020).

Declaration of conflicting interests

The authors declare that there is no conflict of interest.

Acronyms

BTR li-ion battery
CII carbon intensity index
CMB combustion
DF-ICE dual fuel engine
DISC battery discharge
EEDI energy efficiency design index
EEXI energy efficiency existing ship index
EGN exhaust gas NO_x content
ELEC electricity
eLNG synthetic liquified natural gas
EM electric machine
eMDO synthetic marine diesel oil
GRID vessel electricity grid
H2 hydrogen
H2-CMB engine modification for hydrogen combustion
H2-ICE combustion of hydrogen in an internal combustion engine
H2-PEM Electrochemical conversion of hydrogen to electricity in proton exchange membrane fuel cell
H2-RF feed of hydrogen to an internal combustion engine
H2G pressurized hydrogen tank
H2L liquid hydrogen tank
HFO heavy fuel oil
HFOL heavy fuel oil tank

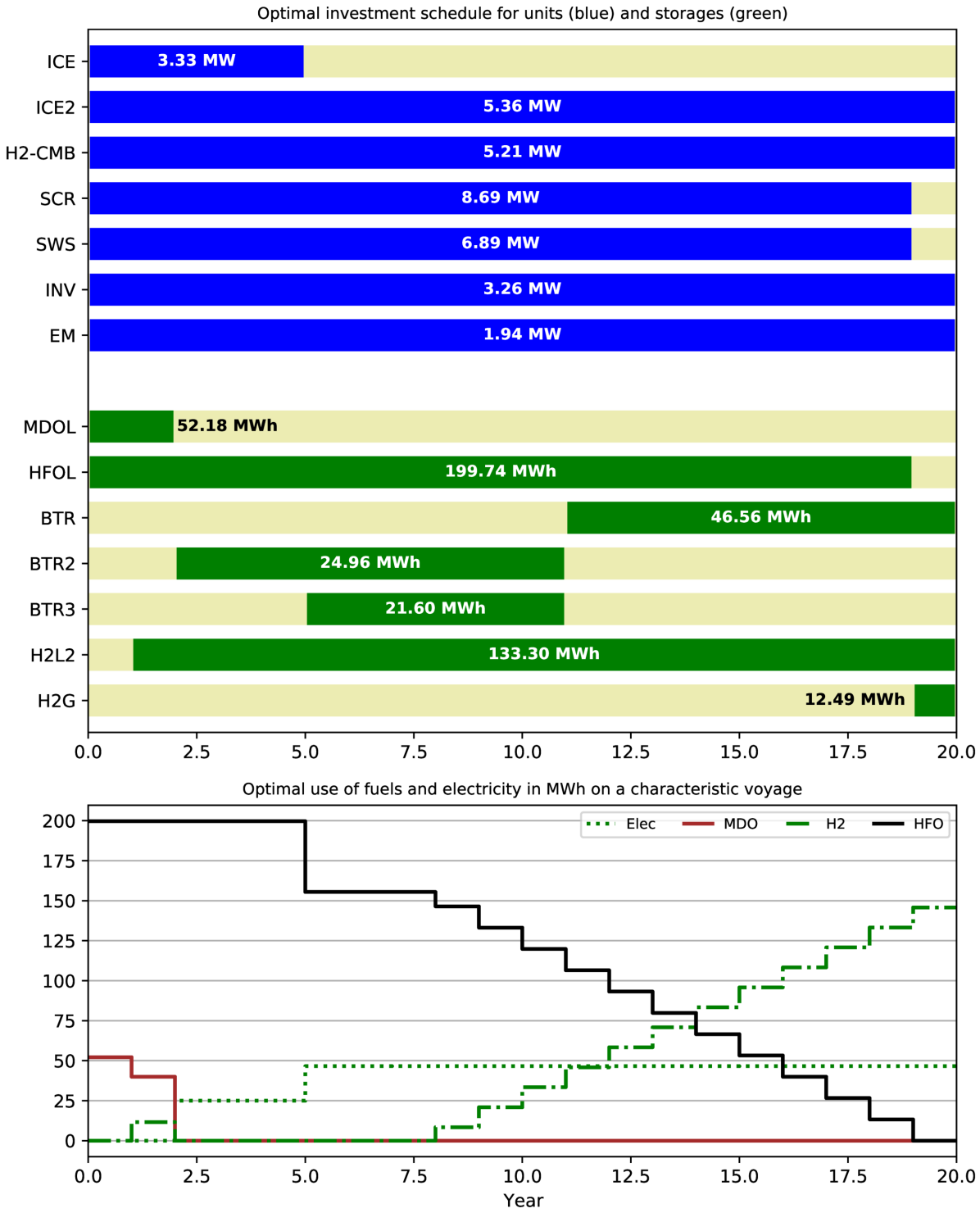

Figure 11. Optimal investment and fuel use plan for the CO_2 emission limit scenario with flexible configuration (P2).

ICE medium speed diesel engine
INV power electronics
LNG liquified natural gas
LNG-ICE combustion of liquified natural gas in an internal combustion engine
LNGL liquified natural gas tank
MDO marine diesel oil
MDO-ICE combustion of marine diesel oil in an internal combustion engine
MDOL marine diesel oil tank
MILP mixed integer linear programming
MTH methanol
MTH-CMB engine modification for methane combustion
MTHL methanol tank
N-CLN removal of NO_x from exhaust gas
NH3 ammonia
NH3-CMB engine modification for ammonia combustion
NH3L ammonia tank
NOX NO_x
PEMFC proton exchange membrane fuel cell stack
PEM-AUX auxiliary functions of a proton exchange membrane fuel cell

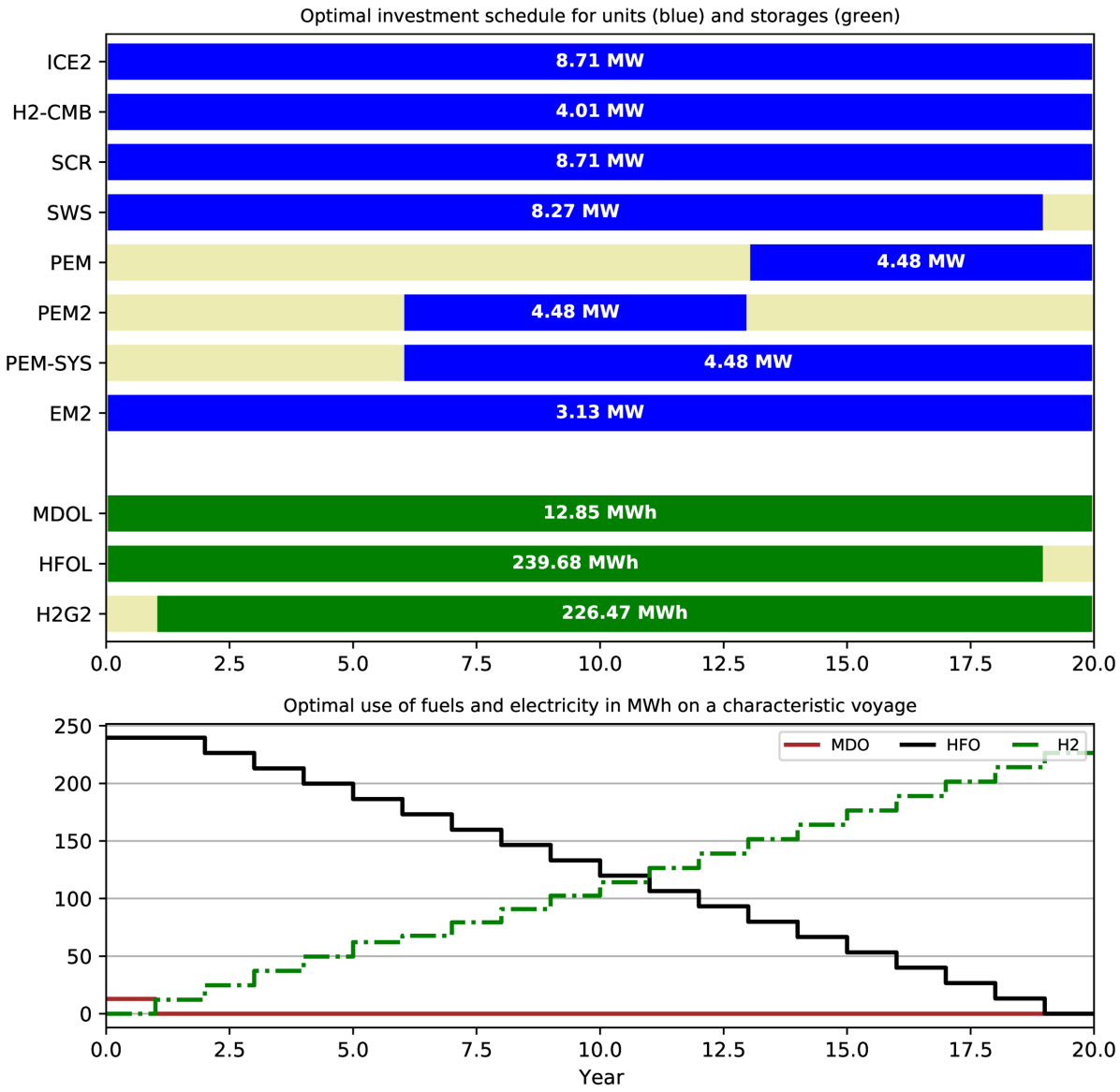

Figure 12. Optimal investment and fuel use plan for the CO_2 emission limit scenario with batteries excluded (P3).

PEM-SYS auxiliary components for proton exchange membrane fuel cell
PROP propeller shaft mechanical energy
PTI power take-in
PTO power take-off
RF fuel processing
S-CLN removal of SO_x from exhaust gas
SCR selective catalytic reduction
SO solid oxide
SO-AUX auxiliary functions of a solid oxide fuel cell
SO-SYS auxiliary components for solid oxide fuel cell
SOFC solid oxide fuel cell stack
TCO total cost of ownership

References

1. IRENA. Renewable energy options for shipping. https://www.irena.org/-/media/Files/IRENA/Agency/Publication/2015/IRENA_Tech_Brief_RE_for-Shipping_2015.pdf, 2015. [Online; accessed 01-February-2021].
2. Sofiev M, Winebrake J, Johansson L et al. Cleaner fuels for ships provide public health benefits with climate tradeoffs. *Nat Commun* 2012; 406(9). doi.org/10.1038/s41467-017-02774-9.
3. IMO. Strategy on the reduction of GHG emissions from ships. https://wwwcdn.imo.org/localresources/en/OurWork/Environment/Documents/ResolutionMEPC.304(72)_E.pdf, 2018. [Online; accessed 24-February-2021].
4. European Commission. Emission trading - putting a price on carbon. https://ec.europa.eu/commission/presscorner/detail/en/qanda_21_3542, 2021. Accessed July 20, 2021.
5. Balcombe P, Brierley J, Lewis C et al. How to decarbonise international shipping: Options for fuels, technologies and policies. *Energy Conversion and Management* 2019; 182: 72–88. https://doi.org/10.1016/j.enconman.2018.12.080. https://www.sciencedirect.com/science/article/pii/S0196890418314250.
6. DNV GL. Energy transition outlook 2020: Maritime forecast to 2050, 2020.

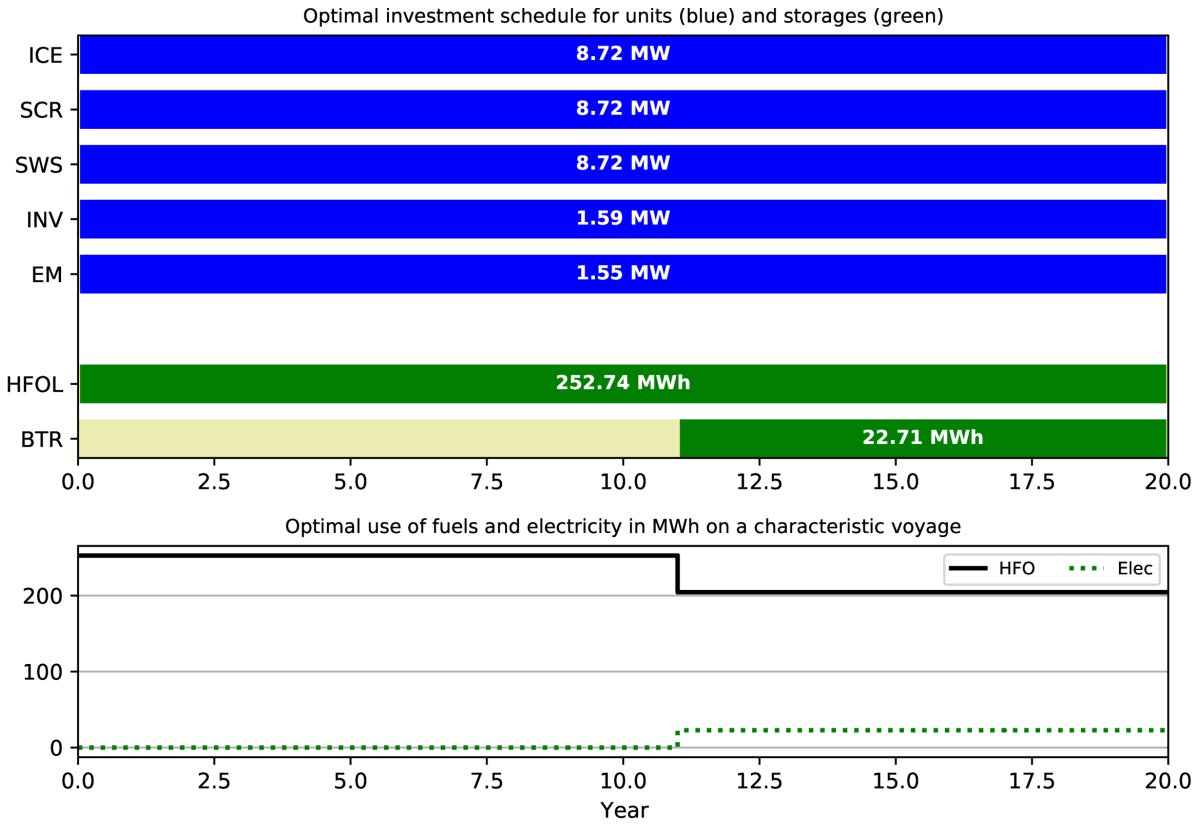

Figure 13. Optimal investment and fuel use plan for the CO_2 pricing problem (P4).

7. Schwartz H, Gustafsson M and Spohr J. Emission abatement in shipping – is it possible to reduce carbon dioxide emissions profitably? *Journal of Cleaner Production* 2020; 254: 120069. https://doi.org/10.1016/j.jclepro.2020.120069. https://www.sciencedirect.com/science/article/pii/S0959652620301165.
8. Baldi F, Brynolf S and Marechal F. The cost of innovative and sustainable future ship energy systems.
9. Mestemaker B, van den Heuvel H and Castro BG. Designing the zero emission vessels of the future: Technologic, economic and environmental aspects. *International Shipbuilding Progress* 2020; 67(1): 5–31. 10.3233/isp-190276. https://doi.org/10.3233/isp-190276.
10. Gaspar HM, Balland O, Aspen DM et al. Assessing air emissions for uncertain life-cycle scenarios via responsive systems comparison method. *Proceedings of the Institution of Mechanical Engineers, Part M: Journal of Engineering for the Maritime Environment* 2015; 229(4): 350–364. 10.1177/1475090214522218.
11. Solem S, Fagerholt K, Erikstad SO et al. Optimization of diesel electric machinery system configuration in conceptual ship design. *Journal of Marine Science and Technology* 2015; 20(3): 406–416. 10.1007/s00773-015-0307-4. https://doi.org/10.1007/s00773-015-0307-4.
12. Winebrake JJ, Corbett JJ, Wang C et al. Optimal fleetwide emissions reductions for passenger ferries: An application of a mixed-integer nonlinear programming model for the New York – New Jersey Harbor. *Journal of the Air & Waste Management Association* 2005; 55(4): 458–466. 10.1080/10473289.2005.10464642. https://doi.org/10.1080/10473289.2005.10464642. https://doi.org/10.1080/10473289.2005.10464642.
13. Balland O, Erikstad SO and Fagerholt K. Optimized selection of air emission controls for vessels. *Maritime Policy & Management* 2012; 39(4): 387–400. 10.1080/03088839.2012.689877.
14. Balland O, Erikstad SO and Fagerholt K. Concurrent design of vessel machinery system and air emission controls to meet future air emissions regulations. *Ocean Engineering* 2014; 84: 283 – 292. https://doi.org/10.1016/j.oceaneng.2014.04.013. http://www.sciencedirect.com/science/article/pii/S0029801814001437.
15. Lagemann B, Lindstad E, Fagerholt K et al. Optimal ship lifetime fuel and power system selection. *Transportation Research Part D: Transport and Environment* 2022; 102: 103145. https://doi.org/10.1016/j.trd.2021.103145. https://www.sciencedirect.com/science/article/pii/S1361920921004405.
16. Erikstad SO. Design for modularity. In Papanikolaou A (ed.) *A Holistic Approach to Ship Design: Volume 1: Optimisation of Ship Design and Operation for Life Cycle*. Springer, 2019. pp. 329–356.
17. Choi M, Erikstad SO and Chung H. Operation platform design for modular adaptable ships: Towards the configure-to-order strategy. *Ocean Engineering* 2018; 163: 85–93. https://doi.org/10.1016/j.oceaneng.2018.05.046. https://www.sciencedirect.com/science/article/pii/S0029801818309065.
18. Baldi F, Moret S, Tammi K et al. The role of solid oxide fuel cells in future ship energy systems. *Energy* 2020; 194: 116811. https://doi.org/10.1016/j.energy.2019.116811. https://www.sciencedirect.com/science/article/pii/S036054421932506X.

19. Kondili E, Pantelides C and Sargent R. A general algorithm for short-term scheduling of batch operations — i. milp formulation. *Computers & Chemical Engineering* 1993; 17(2): 211 – 227. https://doi.org/10.1016/0098-1354(93)80015-F. http://www.sciencedirect.com/science/article/pii/009813549380015F. An International Journal of Computer Applications in Chemical Engineering.
20. Pantelides CC. Unified frameworks for optimal process planning and scheduling. In *Proceedings on the second conference on foundations of computer aided operations*. pp. 253–274.
21. Floudas CA and Lin X. Mixed integer linear programming in process scheduling: Modeling, algorithms, and applications. *Annals of Operations Research* 2005; 139(1): 131–162. 10.1007/s10479-005-3446-x. https://doi.org/10.1007/s10479-005-3446-x.
22. Manne A. On the job-shop scheduling problem. *Operations Research* 1960; 8(2): 219–223. https://EconPapers.repec.org/RePEc:inm:oropre:v:8:y:1960:i:2:p:219-223.
23. Bowman EH. The schedule-sequencing problem. *Operations Research* 1959; 7(5): 621–624. http://www.jstor.org/stable/167010.
24. Horvath S, Fasihi M and Breyer C. Techno-economic analysis of a decarbonized shipping sector: Technology suggestions for a fleet in 2030 and 2040. *Energy Conversion and Management* 2018; 164: 230–241. https://doi.org/10.1016/j.enconman.2018.02.098. https://www.sciencedirect.com/science/article/pii/S0196890418302152.
25. AIMMS. Aimms modeling guide - integer programming tricks. Technical report, 2018. https://documentation.aimms.com/_downloads/AIMMS_modeling.pdf. Accessed: 13 March 2022.
26. ABB. Energy sources and carriers: pathways to compliance, 2020. https://new.abb.com/news/detail/66550/energy-sources-and-carriers-pathways-to-compliance. Accessed: 13 March 2022.
27. MAN. Batteries on board ocean-going vessels. https://www.man-es.com/docs/default-source/marine/tools/batteries-on-board-ocean-going-vessels.pdf?sfvrsn=deaa76b8_14, 2020. [Online; accessed 01-February-2021].
28. Ritari A, Huotari J, Halme J et al. Hybrid electric topology for short sea ships with high auxiliary power availability requirement. *Energy* 2020; 190: 116359. https://doi.org/10.1016/j.energy.2019.116359. https://www.sciencedirect.com/science/article/pii/S0360544219320547.
29. Wartsila Corporation. https://www.wartsila.com/media/news/05-05-2020-wartsila-gas-engines-to-burn-100-hydrogen-2700995. https://www.wartsila.com/media/news/05-05-2020-wartsila-gas-engines-to-burn-100-hydrogen-2700995, 2020. [Accessed 8 February 2022].
30. EMSA European Maritime Safety Agency. Study on the use of fuel cells in shipping. Technical report, 2017.
31. Bacher H and Albrecht P. Evaluating the costs arising from new maritime environmental regulations, 2013. https://www.traficom.fi/sites/default/files/14262-Trafi_Publications_24-2013_-_Evaluating_the_costs_arising_from_new_maritime_environmental_regulations.pdf. Accessed: 13 March 2022.
32. den Boer E and Hoen M. Scrubbers - an economic and ecological assessment. https://www.nabu.de/downloads/150312-Scrubbers.pdf, 2015. Accessed: 13 March 2022.
33. Ship and Bunker. Rotterdam bunker prices. https://shipandbunker.com/prices/emea/nwe/nl-rtm-rotterdam, 2021. Accessed: 8 February 2022.
34. Lloyd's Register. Techno-economic assessment of zero-carbon fuels. Technical report, 2020.
35. Geertsma R, Negenborn R, Visser K et al. Design and control of hybrid power and propulsion systems for smart ships: A review of developments. *Applied Energy* 2017; 194: 30–54. https://doi.org/10.1016/j.apenergy.2017.02.060. https://www.sciencedirect.com/science/article/pii/S0306261917301940.